Available online at www.sciencedirect.com

SciVerse ScienceDirect

Ceramics International 39 (2013) 3657–3662

CERAMICS INTERNATIONAL

www.elsevier.com/locate/ceramint

Effects of Sn on the microstructure and dielectric properties in $BaTiO_3$-based ceramics

Jing Wang[a,b,*], Shenglin Jiang[a], Dan Jiang[b], Tingwei Wang[b], Hao Yao[b]

[a]*Department of Electronic Science and Technology, Huazhong University of Science and Technology, Wuhan 430074, China*
[b]*College of Chemistry and Environmental Science, HeBei University, Baoding 71002, China*

Received 8 July 2012; received in revised form 8 October 2012; accepted 12 October 2012
Available online 24 October 2012

Abstract

$Ba_{0.985}Bi_{0.01}TiO_3$–$BaTi_{1-x}Sn_xO_3$ powders were synthesized by a two-step soft chemical method. Ceramics with core–shell structure could be easily obtained by using these uniformly distributed powders. The ceramics not only satisfied the requirement of EIA-X8R specification, but also were near to that of EIA-X9R specification. Microstructural evaluation conducted by X-ray diffraction and scanning electron microscopy confirmed the hierarchical structure of the ceramic grains. The shape of the ε–T curves near the dielectric peak became broad when x increased from 0.001 to 0.02. The permittivity of $Ba_{0.985}Bi_{0.01}TiO_3$–$BaTi_{0.98}Sn_{0.02}O_3$ ceramic was ~23,000, $\Delta C/C_{20\,^\circ C}$ was −15%, 14.4% and −15% at −55 °C, 120 °C and 170 °C, respectively, and the dielectric loss was 0.5. The results showed that the content of Sn had a strong impact on the diffusion and the dielectric properties of the ceramics.

Keywords: Barium titanate; Ceramic matrix composites; Chemical inhomogeneity; Dielectric materials

1. Introduction

The understanding of ABO_3 perovskite-type oxides is a very active research area with great relevance to both fundamental- and application-related issues, often related to their dielectric and ferroelectric properties [1]. Ceramic components based on $BaTiO_3$ (BT) are the most extensively studied dielectric materials due to their large relative permittivity ($\varepsilon \sim 1000$–2000) and high electrical resistivity ($\rho \sim 10^{12}\,\Omega\,cm$) at room temperature, combined with the ability to control all these properties by chemical doping [2]. For example, Hennings and Rosenstein [3] found that incorporation of the single-doped Bi^{3+} increased the Curie temperature of $BaTiO_3$. Bismuth-based dielectric ceramics have been broadly studied for its relatively low sintering temperature (less than 1000 °C) and high dielectric constant [4,5]. Barium titanate doped with Sn shows improved dielectric performance, i.e., very high permittivity, even higher than that of Zr-doped $BaTiO_3$ [6,7].

Electric components are facing the challenge of working under high temperatures. X7R-type MLCCs with upper working temperature of 125 °C have not been competent in harsh conditions. Therefore, recently, much attention has been paid to the EIA X8R specification (−55 °C to 150 °C, $\Delta C/C_{25\,^\circ C} \leq 15\%$) [8,9]. The formation of core–shell structure is the key point of $BaTiO_3$-based MLCC ceramics with high temperature stability. However, traditional methods are always preparing $BaTiO_3$-based particles with paraelectric shell, which results in the decrease of permittivity. It is known that chemical coating route is useful for producing materials with core–shell structure [10]. Compared with the solid mixing process, chemical coating is more powerful to obtain $BaTiO_3$-based MLCC powders with grain size less than 100 nm [11].

With the trend for increasing the volumetric efficiency of next generation MLCCs, the thickness of the ceramic capacitor layer needs to be further reduced ($< 1\,\mu m$), calling for the utilization of the nano-sized $BaTiO_3$ powder as starting material. However, the clear advantages of nanopowders are often neglected by the increasing

*Corresponding author at: Department of Electronic Science and Technology, Huazhong University of Science and Technology, Wuhan 430074, China. Tel.: +86 2787542693.
E-mail address: jslhust@gmail.com (J. Wang).

0272-8842/$ - see front matter © 2012 Elsevier Ltd and Techna Group S.r.l. All rights reserved.
http://dx.doi.org/10.1016/j.ceramint.2012.10.195

tendency of hard agglomerate formation, as the particle sizes are decreased below 100 nm. Thus it is important for uniformity to be effectively controlled as well as grain size [12,13]. Especially, excellent dispersion status of nano-$BaTiO_3$ particles is strongly demanded in the chemical coating process, because the agglomerates of $BaTiO_3$ particles will affect coating coverage, cause a collapse in the core–shell structure and deteriorate the dielectric properties. On account of these problems, it is difficult to fulfill the fabrication of ultrafine-grained ceramics with a core–shell structure. However, in previous papers, the grain size of $BaTiO_3$ ceramics with core–shell structure was over 400 nm, which cannot satisfy the developing trend of MLCCs with ultrafine ceramic grains below 200 nm [14–16]. As the traditional ball milling method cannot completely break soft agglomerates of nanoparticles and the uniform coverage during the coating process cannot be guaranteed, an effective dispersing route is strongly needed to satisfy the production of next generation MLCCs.

In this paper, $Ba_{0.985}Bi_{0.01}TiO_3$–$BaTi_{1-x}Sn_xO_3$ (BBT–BTS) powders were prepared by the solution-based method. The solution-based method has numerous advantages, including low processing temperatures, excellent compositional control, homogeneous distribution, small grain size and low cost. Ceramic powders with core–shell structure were synthesized, which is comprised of $Ba_{0.985}Bi_{0.01}TiO_3$ (BBT) as core and $BaTi_{1-x}Sn_xO_3$ (BTS) as shell, with the core/shell ratio of 4:6. Due to different Curie temperatures for BBT and BTS, there are two Curie peaks at high-temperature region and low-temperature region in the whole scope of working temperature. The temperature stability will be greatly improved after multiplying of those Curie peaks, presenting the multi-peak effect. Meanwhile, the permittivity of the material can maintain a high level by the incorporation of Bi and Sn. In the present investigation, the powders and ceramic of BBT–BTS with different Sn contents were characterized, and the dielectric properties were thus measured.

2. Experimental procedure

2.1. Preparation of BBT powder [17]

The BBT powders studied were prepared by the liquid-state method with Bi_2O_3, $TiCl_4$ and $Ba(OH)_2 \cdot 8H_2O$ (AR 99.0% China) as raw materials. Firstly, $TiCl_4$ was hydrolyzed in stoichiometric Bi_2O_3 hydrochloric acid solution to form a transparent solution. Then $Ba(OH)_2 \cdot 8H_2O$ was dissolved in boiling water and mixed with the above solution in a flask to form a homogeneous solution. Secondly, the mixture was heated to 95–100 °C by a heating jacket with vigorous and continuous stirring for 4 h. The reaction product then was obtained after washing and drying in the air.

2.2. Preparation of BBT–BTS powder

$SnCl_4$, $TiCl_4$, $Ba(OH)_2 \cdot 8H_2O$ (AR 99.0% China) and the as-prepared BBT were used as starting materials. Firstly, $TiCl_4$ was hydrolyzed in stoichiometric $SnCl_4$ hydrochloric acid solution, and then mixed with $Ba(OH)_2$ boiling water solution in a flask to form a homogeneous solution with stirring. Secondly, BBT was put into the three-necked flask and mixed with the solution together and was made to react at 95–100 °C for 4 h. Then $BaTi_{1-x}Sn_xO_3$ (x=0.001, 0.002, 0.005, 0.01, 0.02, 0.05, 0.1 BTS) would grow at the surface of BBT, because the similarity of their geometrical structure, BBT can act as seed crystal to induce the growth of BTS on the surface. It will be proved by the following characterizations. The products which were denoted as BBTBTS-1, BBTBTS-2, BBTBTS-3, BBTBTS-4, BBTBTS-5, BBTBTS-6, BBTBTS-7 respectively, were obtained after drying in the air.

2.3. Preparation of BBT–BTS ceramics

The prepared ceramic powders were pressed into discs (20 mm in diameter and 2 mm in thickness) using 8 wt% PVA as a binder. After discharging binder, the disks were finally fired at 1100 °C for 1 h in air. Silver paste was fired on both sides of the samples at 550 °C for 10 min as electrodes.

Dielectric measurements of the samples were performed by using a LCR meter at 1 kHz in the temperature range from −55 °C to 180 °C. Phase analysis was carried out by X-ray diffraction (XRD) technique using the Cu Kα radiation of D8 Advance. Scanning electron micrographs (SEM) were recorded with a Jeol 940 A electron microscope. A point-to-point nano-analysis has been done using Scanning Transmission Electron Microscope (STEM) with Energy Dispersive X-ray Spectroscopy (EDX) facility.

3. Results and discussion

Nanoparticles are more subject to dispersive force due to its high surface energy, which enhance the agglomeration behavior of this class of particles. A detailed investigation of particle size distribution can predict the dispersion and consolidation behavior of nanopowders. During fabrication, agglomeration leads to interparticle and interagglomerate pores and form inhomogeneous microstructure.

Fig. 1a shows the size distribution of BBT powders. The average grain size could be controlled below 75 nm with even distribution, which is one of the reasons for the homogeneous core–shell structure grain. As shown in Fig. 1b, BBTBTS-5, which utilized BBT as starting material, exhibits a uniform microstructure with the average grain size of 345 nm. Most of the grains are in the size range of 300–400 nm, and few big grains can be found. Additionally, another important reason for such well-distributed microstructure of BBTBTS-5 is that it is synthesized by BTS-5 growth on the BBT surface though

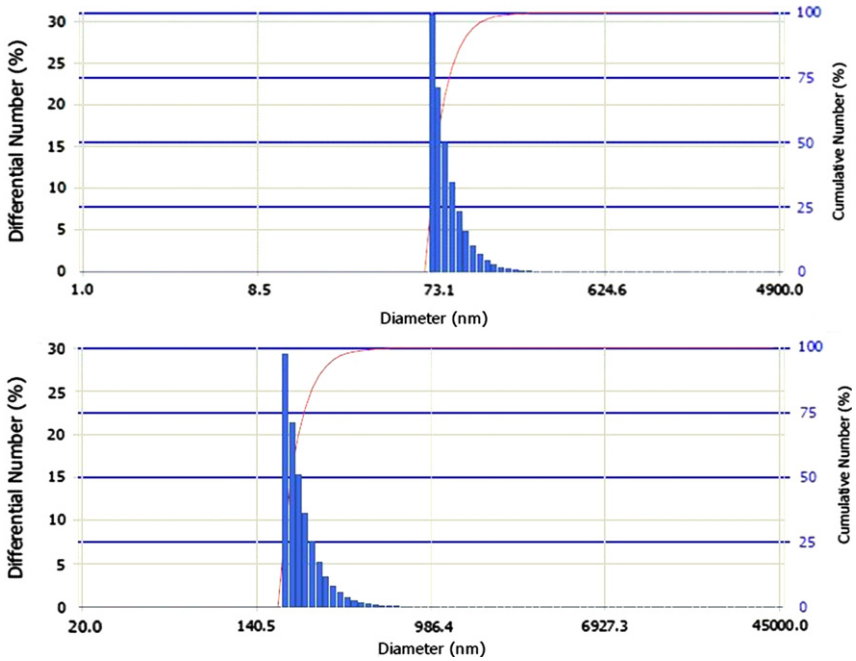

Fig. 1. Grain size distribution of BBT (a) and BBTBTS-5 prepared by the aqueous chemical coating process (b).

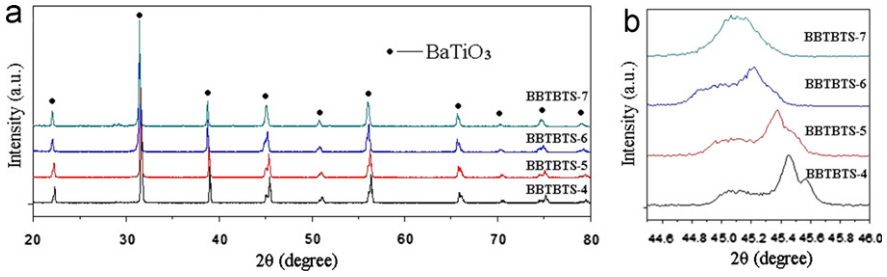

Fig. 2. X-ray diffraction patterns of BBTBTS ceramics doped with different contents of Sn.

the aqueous method. By the conventional method, particles of the additive oxides are mostly in submicrometer scale. It causes a poor dispersion of the additives around $BaTiO_3$ particles because the size of BT particles is very small. Therefore, it gives rise to an inhomogenous concentration distribution of additives around BT particles. In some high-additive concentration regions, the additive elements diffuse deeply into BT lattices and a solid solution is form. It indicates that the aqueous method conduces to better dispersion of the additives around BT particles because of the ionic scale growth of BTS on the BBT grain surface. Consequently, the well dispersion of BTS around BBT powders is beneficial for the formation of the core–shell structure and the preparation of ceramics with high performance.

Fig. 2a presents the X-ray diffraction (XRD) patterns for synthesized compositions measured at room temperature (RT). These XRD patterns are measured on the sintered ceramic pellets. As shown, there is no trace of secondary peak, which suggests the formation of homogeneous solid solution for all the compositions with perovskite phase. Besides, it can be also seen that the peaks shifts to a small angle with the increase of x, which is attributed that Sn^{4+} (0.071 nm) with large ions radius substitute Ti^{4+} (0.068 nm). In Fig. 2b, two (002) peaks at the same position are shown, which indicates that BBT and BTS-4 coexist in the ceramics. With the increase of Sn content, the two overlapping peaks merge into one peak, which predicts that the two phases diffuse into each other. The diffusion is deepened with more Sn modification. When the content of Sn is more than 0.1 at%, (200) and (002) peaks merge into a broad symmetrical peak, which shows pseudocubic symmetry. It suggests that BBT and BTS-7 have diffused into each other to form a solid solution with chemical homogeneity.

Fig. 3a illustrates STEM/EDX point-to-point analysis across the diameter of grain for BBTBTS-5. The result suggests that the content of Bi^{3+} is higher and the content of Sn^{4+} is lower at the grain core than that of those at grain shell, which indicates that BBT is coated by BTS-5.

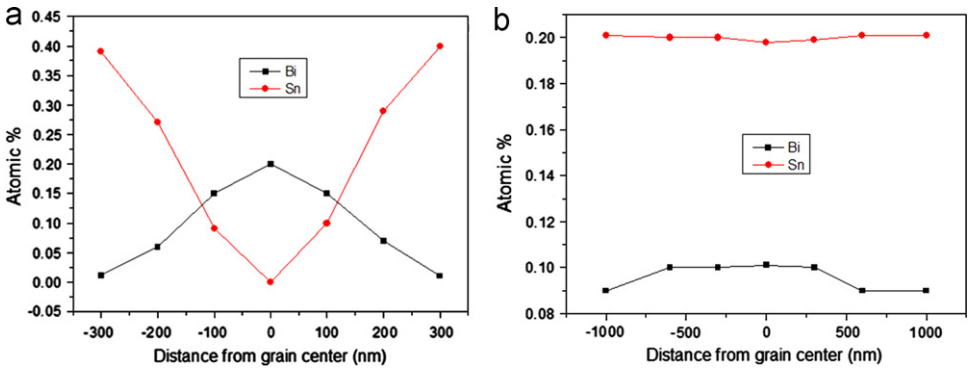

Fig. 3. EDX composition profile across the diameter of grain for BBTBTS-5 (a) and BBTBTS-6 (b).

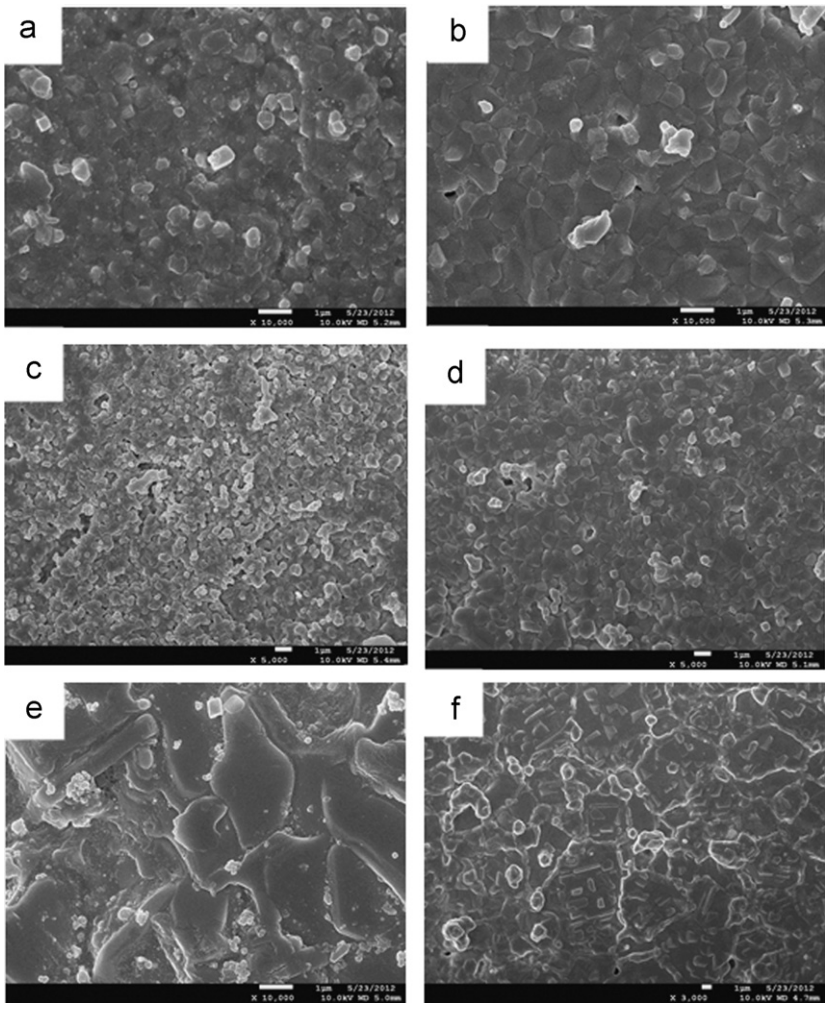

Fig. 4. SEM images of BBTBTS ceramics doped with different contents of Sn (a) 0.001, (b) 0.005, (c) 0.01, (d) 0.02, (e) 0.05, and (f) 0.1.

However, in Fig. 3b, the STEM/EDX point-to-point analysis for BBTBTS-6 shows two straight lines. The result suggests that the grain core and the shell share the same content of Bi^{3+} and Sn^{4+}, respectively, which indicates that BBT and BTS-6 have diffused into each other homogeneously.

In Fig. 4a, it can be seen that the blurred boundaries suggest the formation of liquid phase in the sintering process. It results from the low melt point of Bi_2O_3 (820 °C). When the sintering temperature is higher than 820 °C, Bi_2O_3 will melt, volatilize, and then deposit at boundaries when sample is cooled down. From Fig. 4b and c, the grain boundaries become more clear, which indicates that the segregation of Bi^{3+} is depressed with increasing Sn content. The quantity of liquid phase at boundaries

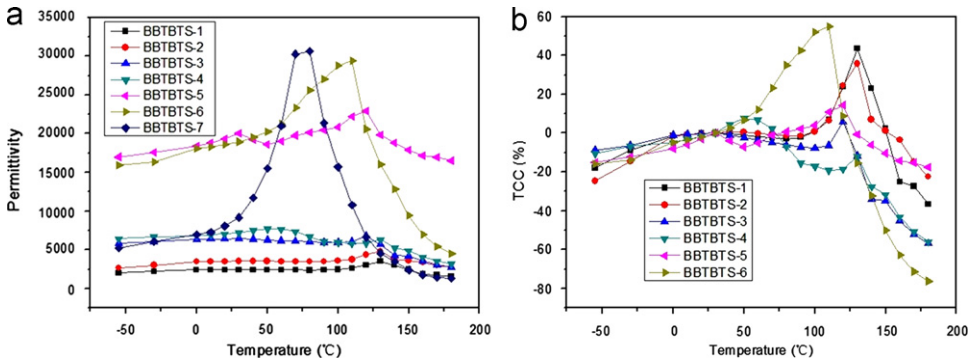

Fig. 5. Temperature dependence of permittivity (a) and temperature coefficient of capacity (b) for different samples.

decreases, and disappears when x is higher than 0.005. Sn ions at shells are associated with point defects and lattice distortion, which will yield strain energy. On account of the strain energy, the formation energy of oxygen vacancies can be lowered to a certain extent and the grain-boundary diffusion coefficient is enhanced, as shown in Fig. 4b–d. The extent of diffuseness between BBT and BTS increases as more Sn is added. It is noticed that the grain size increases abnormally and shows a nonuniform distribution when the content of Sn is more than 0.05 (Fig. 4e and f). Modified ceramic has more defects as more Sn is added. A large amount of defect improves the mass transport process, resulting in the diffusion between BBT and BTS and the growth of grains.

Fig. 5a and b shows the temperature dependence of dielectric constant and the temperature coefficient of capacity in the range of −55 to 180 °C, which was measured at 1 kHz for the compositions of BBTBTS with various Sn contents. It is found that the dielectric constant increases with the increase of Sn content. Based on the discussion above, Sn addition results in point defects and lattice distortion, which yield the internal stress. The internal stresses are responsible for the permittivity increase according to Arlt [18]. It is also noticed that the dielectric peaks of BBTBTS-1 to BBTBTS-5 are effectively depressed with the increase of BTS content. Besides, the shape of the ε–T curves near the dielectric peak becomes broader with increasing Sn content. Especially, BBTBTS-5 shows that the temperature coefficient of capacity is −15%, 14.4%, and −15% at −55, 120, and 170 °C, respectively, which not only meets the requirement of X8R specification, but also is near to that of X9R specification. The best temperature stability of dielectric constant can be expressed semi-quantitatively using the Lichtenecker formula, $\log \varepsilon = V_1 \log \varepsilon_1 + V_2 \log \varepsilon_2$, in which ε of the ceramic is determined by both core part and shell part. So, low TCC can be obtained [16,19]. In addition, the substitution of Sn induces the compositional inhomogeneity, which results in the multiphase character over a relatively wide temperature range. The combination of property overlying and constituent fluctuations contributes to the improvement of temperature stability of dielectric properties. For BBTBTS-6 and BBTBTS-7, the Tc shifts to 110 and 80 °C, respectively, and the peaks become narrower. The narrowing and enhancing of peak is found to increase with the Sn content in the base matrix. The reducing of Tc and temperature stability are attributed to a chemical homogeneity of microstructure and the disappearance of diffuse phase transition (DPT).

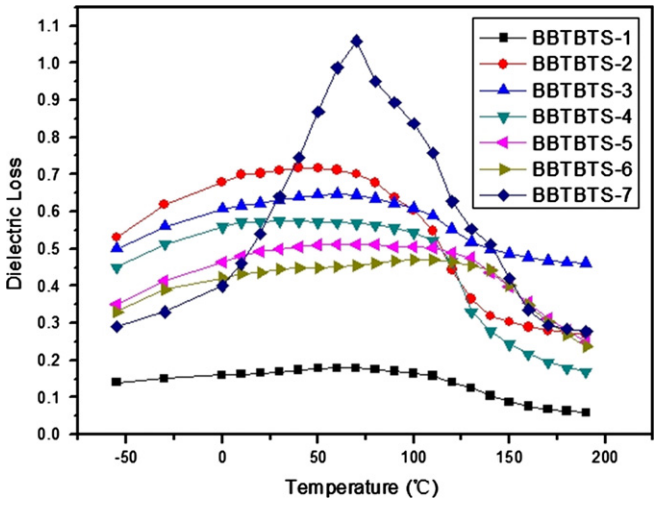

Fig. 6. Temperature dependence of dielectric loss for different samples.

Fig. 6 shows the temperature dependence of dielectric loss for samples with various Sn contents. When $x=0.001$, a mount of Bi_2O_3 deposits at grain boundaries, hindering the electronic hopping among grains. It makes a lower dielectric loss. The increase of dissipation for BBTBTS-2 attributes to the disappearance of Bi_2O_3 segregation and low density of the ceramic. However, with the increase of Sn content, the dissipation decreases. Because Sn^{4+} is chemically more stable than Ti^{4+} and the substitution of Ti with Sn would depress the conduction by electronic hopping between Ti^{4+} and Ti^{3+}, thus inducing a decline of leakage current. When $x=0.1$, too much defects are formed because of the much higher doping amounts. The defects provide many channels for electronics to migrate, resulting in a large dissipation of 1.06.

4. Conclusions

The hierarchy-structural $Ba_{0.985}Bi_{0.01}TiO_3$–$BaTi_{1-x}Sn_xO_3$ powders are synthesized by a soft chemical method. After

proper sintering, ceramics with core–shell structure can be easily obtained. The dielectric constant improves with the increase of Sn content. But, when the content of Sn is too much, chemical homogeneity microstructure appears, which results in high TCC and dissipation. The dielectric stability of $Ba_{0.985}Bi_{0.01}TiO_3$–$BaTi_{1-x}Sn_xO_3$ ceramic is significantly improved when x is 0.02, due to composition inhomogeneity and structure defects. The dielectric properties are: $\varepsilon = \sim 23{,}000$, $\tan\delta = 0.5$, $\Delta C/C_{20\,^\circ C}$ at $-55\,^\circ C$, $120\,^\circ C$ and $170\,^\circ C$ are -15%, 14.4% and -15%, respectively.

Acknowledgments

This work is funded by National Science and Technology Support Program (2012BA113B00), National Nature Science Foundation of China (51102102), the Specialized Research Fund for the Doctoral Program of Higher Education of China (20110142120074), Science and Technology Plan Project of Wuhan (201210321103), and Youth Fund of Hebei University (2008Q23).

References

[1] J. Kreisel, B. Noheda, B. Dkhil, Phase transitions and ferroelectrics: revival and the future in the field, Phase Transitions 82 (2009) 633–661.

[2] A. Feteira, D.C. Sinclair, J. Kreisel, Average and local structure of $(1-x)BaTiO_3$–$xLaYO_3$ $(0 \le x \le 0.50)$ ceramics, Journal of the American Ceramic Society 93 (2010) 4174–4181.

[3] D. Hennings, G. Rosenstein, Temperature-stable dielectrics based on chemically inhomogeneous $BaTiO_3$, Journal of the American Ceramic Society 67 (1984) 249–254.

[4] H.C. Ling, M.F. Yan, W.W. Rhodes, High dielectric constant and small temperature coefficient bismuth-based dielectric compositions, Journal of Materials Research 5 (1990) 1752–1762.

[5] D.H. Liu, Y. Liu, S.Q. Huang, X. Yao, Phase structure and dielectric properties of Bi_2O_3–ZnO–Nb_2O_3-based dielectric ceramics, Journal of the American Ceramic Society 76 (1993) 2129–2132.

[6] X.Y. Wei, Y.J. Feng, X. Yao, Dielectric relaxation behavior in barium stannate ferroelectric ceramics with diffused phase transition, Applied Physics Letters 83 (2003) 2031–2033.

[7] N. Horchidan, A.C. Ianculescub, L.P. Curecheriua, F. Tudorachea, V. Musteatac, S. Stoleriub, N. Dragand, D. Crisand, S. Tascua, L. Mitoseriua, Preparation and characterization of barium titanate stannate solid solutions, Journal of Alloys and Compounds 509 (2011) 4731–4737.

[8] L. Zhang, O.P. Thakur, A. Feteira, G.M. Keith, A.G. Mould, D.C. Sinclair, A.R. West, Comment on the use of calcium as a dopant in X8R $BaTiO_3$-based ceramics, Applied Physics Letters 90 (2007) 142914.

[9] M. Du, Y. Li, Y. Yuan, S. Zhang, B. Tang, A novel approach to $BaTiO_3$-based X8R ceramics by calcium borosilicate glass ceramic doping, Journal of Electronic Materials 36 (2007) 1389–1394.

[10] R.Z. Liu, Y.Z. Zhao, R.X. Huang, Y.J. Zhao, H.P. Zhou, Multiferroic ferrite/perovskite oxide core/shell nanostructures, Journal of Materials Chemistry 20 (2010) 10665–10670.

[11] Y.C. Zhang, X.H. Wang, Z.B. Tian, K.H. Hur, L.T. Li, Preparation of BME MLCC powders by aqueous chemical coating method, Journal of the American Ceramic Society 94 (2011) 3286–3290.

[12] C.H. Kim, K.J. Park, Y.J. Yoon, M.H. Hong, J.O. Hong, K.H. Hur, Role of yttrium and magnesium in the formation of core–shell structure of $BaTiO_3$ grains in MLCC, Journal of the European Ceramic Society 28 (2008) 1213–1219.

[13] Z.B. Tian, X.H. Wang, Y.C. Zhang, J. Fang, T.H. Song, K.H. Hur, S. Lee, L.T. Li, Formation of core–shell structure in ultrafine-grained $BaTiO_3$-based ceramics through nanodopant method, Journal of the American Ceramic Society 93 (2010) 171–175.

[14] J. Nishikawa, T. Hagiwara, K. Kobayashi, Y. Mizuno, H. Kishi, Effects of microstructure on the curie temperature in $BaTiO_3$–Ho_2O_3–MgO–SiO_2 system, Japan Journal of Applied Physics 46 (2007) 6999–7004.

[15] C.H. Kim, K.J. Park, Y.J. Yoon, D.S. Sinn, Y.T. Kim, K.H. Hur, Effects of milling condition on the formation of core–shell structure in $BaTiO_3$ grains, Journal of the European Ceramic Society 28 (2008) 2589–2596.

[16] Y.C. Zhang, X.H. Wang, J.Y. Kim, Z.B. Tian, J. Fang, K.H. Hur, L.T. Li, High performance $BaTiO_3$-based BME–MLCC nanopowder prepared by aqueous chemical coating method, Journal of the American Ceramic Society 95 (2012) 1628–1633.

[17] J. Wang, S.L. Jing, D. Jiang, J.J. Tian, Y.L. Li, Y. Wang, Microstructural design of $BaTiO_3$-based ceramics for temperature-stable multilayer ceramic capacitors, Ceramics International 38 (2012) 5853–5857.

[18] G. Arlt, D. Hennings, G. With, Dielectric properties of fine-grained barium titanate ceramics, Journal of Applied Physics 58 (1985) 1619–1625.

[19] H. Wen, X.H. Wang, Z.L. Gui, L.T. Li, Modeling of the core–shell microstructure of temperature-stable $BaTiO_3$ based dielectrics for multilayer ceramic capacitors, Journal of Electroceramics 21 (2008) 545–548.